Macromolecules

ARTICLE

pubs.acs.org/Macromolecules

In Situ NMR and Modeling Studies of Nitroxide Mediated Copolymerization of Styrene and *n*-Butyl Acrylate

Lebohang Hlalele[†] and Bert Klumperman[†,‡,*]

[†]Department of Chemistry and Polymer Science, University of Stellenbosch, Private Bag X1, Matieland 7602, South Africa

[‡]Laboratory of Polymer Chemistry, Eindhoven University of Technology, P.O. Box 513, 5600 MB Eindhoven, The Netherlands

Supporting Information

ABSTRACT: The combination of *in situ* ^{1}H NMR and *in situ* ^{31}P NMR was used to study the nitroxide mediated copolymerization of styrene and *n*-butyl acrylate. The alkoxyamine MAMA-DEPN was employed to initiate and mediate the copolymerization. The nature of the ultimate/terminal monomer units of dormant polymer chains were identifiedand quantified by *in situ* ^{31}P NMR. Simulations of the styrene and *n*-butyl acrylate copolymerization mediated by DEPN were investigated using the Predici software package. The rate coefficients of reversible deactivation of chains with *n*-butyl acrylate as the terminal unit were estimated via parameter estimation studies using Predici. Good correlations were obtained between experimental data and simulated data.

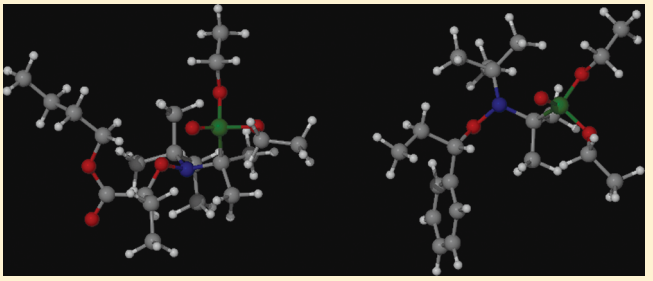

INTRODUCTION

In the past 2 decades, much attention has been focused on copolymerizations due to a wide variety of applications that can be served by copolymers.[1−4] In particular, styrene and *n*-butyl acrylate copolymers obtained via different techniques have been extensively studied and reported.[1,5,6] The use of *in situ* NMR in studies of living radical homo- and copolymerizations has proven to be very powerful.[7−10] Kinetic parameters such as reactivity ratios have been determined from *in situ* ^{1}H NMR data for different systems.[8,9] Information on copolymer composition has also been reported from *in situ* ^{1}H NMR data.[2,9]

In this contribution, we report the use of *in situ* ^{31}P NMR to monitor the copolymerization of styrene and *n*-butyl acrylate. The presence of phosphorus in the nitroxide *N*-*tert*-butyl-*N*-(1-diethoxyphosphoryl-2,2-dimethylpropyl)aminooxyl radical (DEPN, Scheme 1) used to mediate the polymerization allowed for the use of ^{31}P NMR to monitor dormant chains in the copolymerization system. Simulation of the copolymerization of styrene and *n*-butyl acrylate was also carried out using the Predici software package (Version 6.72.3). Validity of the use of k_c^B and k_d^B determined from homopolymerization data in the description of copolymerization kinetics is addressed.

EXPERIMENTAL SECTION

Chemicals. The alkoxyamine2-methyl-2-[*N*-*tert*-butyl-*N*-(1-diethoxyphosphoryl-2,2-dimethylpropyl)-aminooxy]propionic acid (MAMA-DEPN) was synthesized as described in the Supporting Information. Styrene and *n*-butyl acrylate (Plascon Research Centre, University of Stellenbosch) were washed with 10% aqueous solution of sodium hydroxide and then washed with distilled deionized water and dried with anhydrous magnesium sulfate. The respective monomers were then distilled under reduced pressure and stored at low temperatures. Deuterated dimethyl sulphoxide (DMSO-d_6, Cambridge Isotope Laboratories, 99%) and dimethylformamide (DMF, Aldrich) were used as received.

Scheme 1. Nitroxide DEPN and the Corresponding Alkoxyamine MAMA-DEPN Used in the Copolymerization of Styrene and *n*-Butyl Acrylate

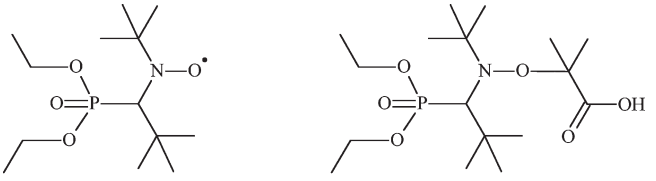

Procedure for the in Situ ^{1}H NMR Monitored Copolymerization. Styrene and *n*-butyl acrylate copolymerizations were followed via *in situ* ^{1}H NMR at 120 °C at different monomer feed compositions in DMSO-d_6. The ^{1}H NMR spectra were recorded on a 400 MHz Varian Unity Inova spectrometer. The ^{1}H NMR spectra were acquired with a 3 μs (40°) pulse width and a 4 s acquisition time. The NMR tube was first inserted into the magnet at 25 °C and the magnet fully shimmed on the sample and a spectrum collected to serve as reference at 25 °C. This was followed by removal of the sample from the magnet and the probe of the magnet was then heated to 120 °C and allowed to stabilize before

Received: May 21, 2011
Revised: July 27, 2011
Published: August 04, 2011

Scheme 2. Structures of Dormant Polymer Chains with *n*-Butyl Acrylate (A) and Styrene (B) as the Terminal Unit to Which the Nitroxide DEPN Moieties Are Attached

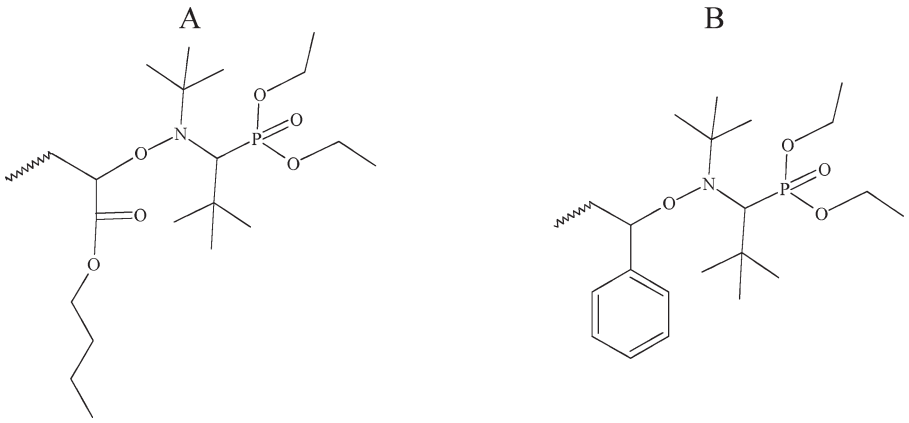

introducing the sample into the cavity of the magnet. After reinsertion of the sample, additional shimming was performed to acquire optimum conditions. The first spectrum was acquired 3−5 min after the reinsertion, followed by periodic spectra acquisition every 2 min for 90 min. Phase correction and baseline correction were performed automatically while integration of the spectra was carried out manually using ACD Laboratories 10.0 1D ^{1}H NMR processor. Concentration profiles were constructed relative to the reference (DMF).

In a typical copolymerization reaction, 30.1 mg of MAMA-DEPN (0.0789 mmol), 0.0722 g of styrene (0.693 mmol), 0.1314 g of *n*-butyl acrylate (1.025 mmol), 20 μL of DMF and 0.3113 g of DMSO-d_6 were thoroughly mixed and introduced into a J-Young type NMR tube. The DMF served as an internal reference material. The reaction mixture was degassed by three freeze−pump−thaw cycles and backfilled with nitrogen gas. The copolymerization was allowed to run for 90 min.

Procedure for the in Situ ^{31}P NMR Monitored Copolymerization. The ^{31}P NMR spectra were acquired with a 4.75 μs (45°) pulse width, a 1.6 s acquisition time, a relaxation delay of 1 s and an average of 23 scans per spectrum. Experimental procedures for the *in situ* ^{31}P NMR monitored copolymerization were identical to those of the *in situ* ^{1}H NMR monitored copolymerization experiments. The spectra were processed manually using ACD Laboratories 10.0 NMR processor.

In a typical copolymerization reaction, 30.3 mg MAMA-DEPN (0.0794 mmol), 0.1191 g styrene (1.1436 mmol), 0.1078 g *n*-butyl acrylate (0.8411 mmol) and 0.3094 g DMSO-d_6 were thoroughly mixed and introduced into a J-Young type NMR tube. The reaction mixture was degassed by three freeze−pump−thaw cycles and backfilled with nitrogen gas. The copolymerization was allowed to run for 90 min.

Modeling. The simulations of the copolymerization were carried out using the Predici software package (version 6.72.3).

RESULTS AND DISCUSSION

The presence of a phosphorus nucleus in the structure of the persistent nitroxide used in this study allowed for use of *in situ* ^{31}P NMR to probe the mechanistic features of styrene/*n*-butyl acrylate copolymerization. Preliminary homopolymerization reactions of styrene and *n*-butyl acrylate monitored via *in situ* ^{31}P NMR were carried out, following the chemical shift of the phosphorus of the nitroxide chain end moiety (Scheme 2). The ^{31}P NMR spectra of dormant species shown in Scheme 2 are shown in Figure 1. In the dormant state, the signal due to phosphorus in which styrene is the terminal unit differs from that

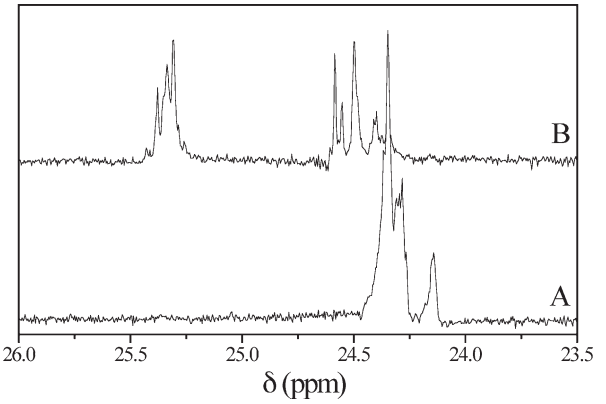

Figure 1. ^{31}P NMR spectra of dormant polymer chains with styrene (B) and *n*-butyl acrylate (A) as terminal units to which the nitroxide DEPN is attached in the respective homopolymerization reactions.

in which *n*-butyl acrylate is the terminal unit of the dormant chain. Thus, in copolymerization reactions the resulting phosphorus peaks can be used to distinguish dormant chains with either styrene or *n*-butyl acrylate as the terminal unit of a dormant polymer chain.

The ^{31}P NMR spectra for the homopolymerizations of styrene and *n*-butyl acrylate are shown in Figure 1. A complex multiplicity of signal peaks in both cases where styrene and *n*-butyl acrylate are terminal units is observed. The multiplicity can be explained by considering that the lone pair on the nitrogen of the nitroxide (in the dormant form) may align with the P═O making the nitrogen an active chiral center and the carbon α to the nitrogen is also a chiral center, such that there can exist the *rac*- or *meso*-forms of the structure. The two ethoxy groups attached to the phosphorus are also not magnetically equivalent. A typical ^{31}P NMR spectrum acquired during the copolymerization of styrene and *n*-butyl acrylate is illustrated by Figure 2, which shows two distinct regions of peaks. From the preliminary *in situ* ^{31}P NMR homopolymerization of both styrene and *n*-butyl acrylate (Figure 1), the regions of peaks in Figure 2 could be assigned. The region labeled "S" is a result of styrene being the terminal unit and the "S + B" region is an overlap of signal peaks

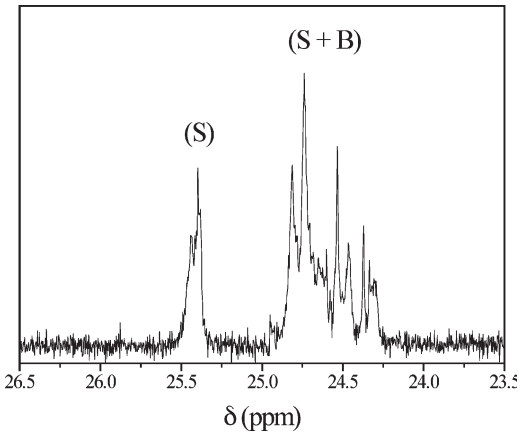

Figure 2. *In situ* ^{31}P NMR spectrum acquired 256 s into the copolymerization of styrene and *n*-butyl acrylate in DMSO-d_6 at 120 °C with the alkoxyamine MAMA-DEPN, at initial feed composition corresponding to $f_S^0 = 0.3$.

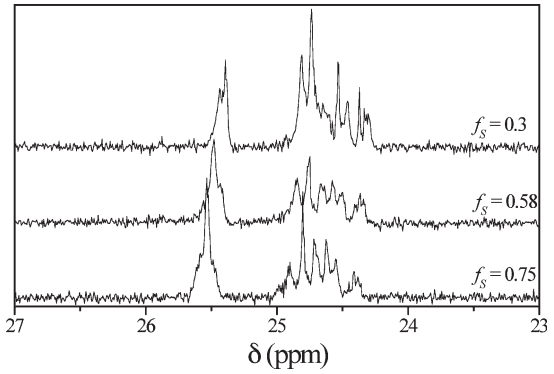

Figure 3. ^{31}P NMR spectra of the styrene/*n*-butyl acrylate copolymerization system at three initial feed compositions indicating signals due to dormant chains with styrene and *n*-butyl acrylate as terminal units.

resulting from styrene and *n*-butyl acrylate being terminal units to which the DEPN is attached.

For the *in situ* ^{31}P NMR homopolymerization of styrene, two regions of peaks were observed and their ratio remained constant throughout the entire polymerization time. With the knowledge of this ratio, the overlapping region (S + B) in Figure 2 could be resolved into two respective constituents, i.e. the contributions from dormant chains with styrene and *n*-butyl acrylate as the terminal units.

To assess the effect of the initial feed composition on the ^{31}P NMR spectrum, *in situ* ^{31}P NMR copolymerizations were conducted at different initial feed compositions. Kelemen et al. reported a significant variation in the ^{15}N NMR spectra as a function of initial feed composition.[11] In Figure 3, the ^{31}P NMR spectra are shown for three different initial feed compositions. The signal at 25.5 ppm due to styrene being the terminal unit, shifts upfield with the decreasing fraction of styrene in the initial feed composition. The change in chemical shift in the signal can be explained by considering the penultimate unit effects. At higher fractions of styrene in the feed, the contribution to the signal at 25.5 ppm is mainly due to the adduct PSS_i-DEPN. As the fraction of styrene in the feed is lowered, there is an increase in adduct of type PBS_i-DEPN, resulting in the shift of the signal.

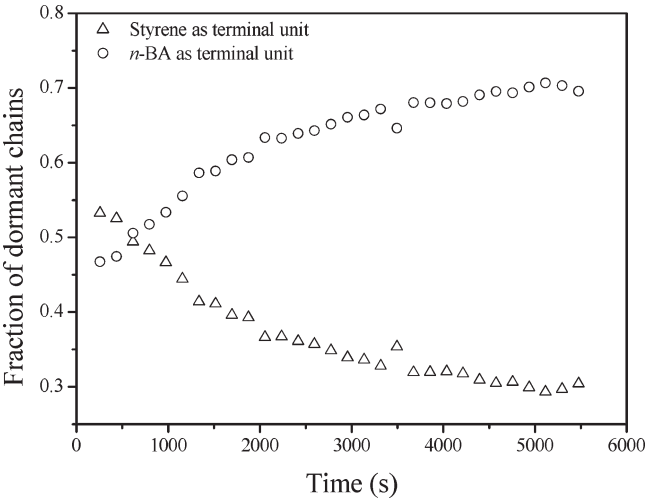

Figure 4. Evolution of the fractions of dormant chains with styrene and *n*-butyl acrylate as the terminal units for a copolymerization with $f_S^0 = 0.3$.

The possibility of the effect of the antepenultimate unit also exists, though it cannot be distinguished from that of the penultimate unit effect from this data. The respective signal intensities in Figure 3 vary with the initial feed composition as would be expected. However subtle, change in the shape of the ^{31}P NMR spectra is observed with varying initial feed composition. This latter observation can be related to the significant change reported in the ^{15}N NMR spectra of styrene/methyl acrylate system as a function of initial feed composition.[11]

Evolution of the fractions of dormant chains with styrene and *n*-butyl acrylate as terminal units for $f_S^0 = 0.3$, is illustrated in Figure 4. At early stages of the reaction, slightly more than 50% of the dormant chains have styrene as the terminal unit. At about 15% overall monomer conversion, the system has an approximately equal number of dormant chains with styrene and *n*-butyl acrylate as the terminal unit. Beyond the 15% conversion, the fraction of dormant chains with *n*-butyl acrylate as the terminal unit gradually increases to a total of about 70%.

At monomer feed compositions below the azeotrope (with respect to styrene), the relative rate of styrene consumption is faster than that of *n*-butyl acrylate. The result is composition drift, which leads to a decrease in the fraction of styrene and an increase in that of *n*-butyl acrylate. As a result, at monomer feed compositions below the azeotrope, the fraction of dormant chains with styrene terminal unit will show a gradual decrease with polymerization time or overall monomer conversion.

Two *in situ* NMR copolymerization experiments were conducted with both samples prepared as identical as possible. One was followed via *in situ* ^{1}H NMR and the other via *in situ* ^{31}P NMR. From the former technique, conversion data was obtained that could be correlated with the terminal unit data from the latter technique. The results are summarized in Figure 5. From Figure 5, the fraction of dormant chains with *n*-butyl acrylate as the terminal unit is illustrated as a function of overall monomer conversion and instantaneous feed composition with respect to *n*-butyl acrylate. With increasing overall monomer conversion, the instantaneous feed composition of *n*-butyl acrylate will increase gradually for copolymerizations conducted with an initial feed composition below the azeotropic feed composition for styrene.

Because of the overlap of peaks in the *in situ* ^{31}P NMR monitored copolymerizations, an alternative method was required to

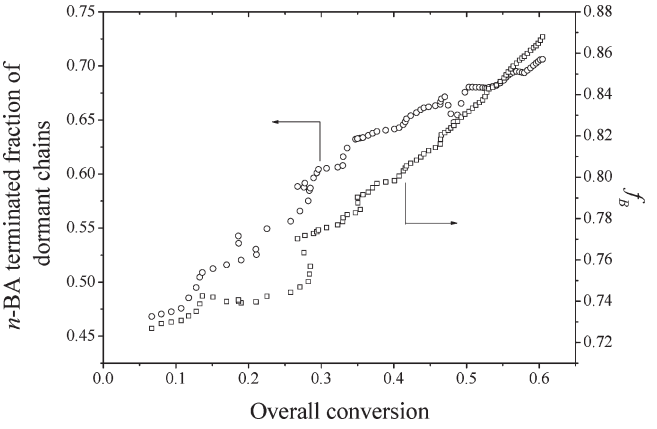

Figure 5. Evolution of the fraction of dormant chain with the *n*-butyl acrylate as the terminal unit and instantaneous feed composition as a function of overall monomer conversion for the copolymerization of styrene and *n*-butyl acrylate with $f_S^0 = 0.3$.

validate the data. Simulations of the styrene/*n*-butyl acrylate were carried out with the Predici software package for comparison with the experimental data. The implicit penultimate unit model (IPUM) was considered in the simulation of the copolymerization process. The terminal unit model (TUM) has been found inadequate in the description of average propagation rate coefficient, and for the purpose of the rate description of copolymerization processes, more comprehensive copolymerization models like the penultimate unit model (PUM) are employed. Before validation of the *in situ* ^{31}P NMR results on tracking the terminal unit of dormant chains, the copolymerization model was tested against experimental data in the feed composition range $0.2 \leq f_S^0 \leq 0.8$. The full copolymerization model description is illustrated by Scheme 3, with the applicable rate coefficients in Table 1.

Figures 6 and 7 illustrate simulated and experimental evolution of styrene and *n*-butyl acrylate concentrations with time. A discrepancy between the experimental and simulated data is observed. Two possible explanations for the observed discrepancy between the experimental and simulated data with regard to monomer concentration profiles are considered. The first explanation involves consideration of penultimate unit effects on activation/deactivation equilibria. The second possible explanation that will be discussed further in this paper involves assessing the validity of the use of k_c^B and k_d^B determined from *n*-butyl acrylate homopolymerizations in kinetic description of copolymerizations. In *n*-butyl acrylate homopolymerization, chain transfer is a well documented phenomenon resulting in coexistence of secondary propagating radicals (SPRs) and tertiary midchain radicals (MCRs).[19−21] In the presence of a free nitroxide, both the SPRs and MCRs can undergo reversible deactivation (Scheme 4).[22]

Because of the reversible deactivation of both the SPR and the MCR, the equilibrium can be described by eq 3, assuming steady state conditions. As a result, one can argue that the equilibrium constant determined from *n*-butyl acrylate homopolymerization is a composite value describing the two processes illustrated in Scheme 4.

$$k_d[\mathrm{P{-}X}] + k_d^t[\mathrm{Q{-}X}] = k_c[\mathrm{P^\bullet}][\mathrm{X}] + k_c^t[\mathrm{Q^\bullet}][\mathrm{X}] \qquad (3)$$

Scheme 3. Implicit Penultimate Unit Model (IPUM) for the Copolymerization of Styrene and *n*-Butyl Acrylate Implemented into the Predici Software Package

RY			⇌	R·	+ Y	k_{act} / k_{deact}
R·	+ S		→	PSS_1·		k_{add}^S
R·	+ B		→	PBB_1·		k_{add}^B
PSS_i·	+ S		→	PSS_{i+1}·		k_p^{SSS}
PSS_i·	+ B		→	PSB_{i+1}·		k_p^{SSB}
PBS_i·	+ S		→	PSS_{i+1}·		k_p^{BSS}
PBS_i·	+ B		→	PSB_{i+1}·		k_p^{BSB}
PBB_i·	+ B		→	PBB_{i+1}·		k_p^{BBB}
PBB_i·	+ S		→	PBS_{i+1}·		k_p^{BBS}
PSB_i·	+ B		→	PBB_{i+1}·		k_p^{SBB}
PSB_i·	+ S		→	PBS_{i+1}·		k_p^{SBS}
PSS_i·	+ Y		⇌	PSS_iY		k_c^S / k_d^S
PBS_i·	+ Y		⇌	PBS_iY		k_c^S / k_d^S
PSB_i·	+ Y		⇌	PSB_iY		k_c^B / k_d^B
PBB_i·	+ Y		⇌	PBB_iY		k_c^B / k_d^B
PSS_i·	+	PSS_i·	→	D		k_{tc}^{SS}
PBB_i·	+	PBB_i·	→	D		k_{tc}^{BB}
PSB_i·	+	PSB_i·	→	D		k_{tc}^{BB}
PBS_i·	+	PBS_i·	→	D		k_{tc}^{SS}
PSS_i·	+	PBB_i·	→	D		k_{tc}^{SB}
PSS_i·	+	PSB_i·	→	D		k_{tc}^{SS}
PSS_i·	+	PBS_i·	→	D		k_{tc}^{SS}
PBB_i·	+	PSB_i·	→	D		k_{tc}^{BB}
PBB_i·	+	PBS_i·	→	D		k_{tc}^{SS}
PSB_i·	+	PBS_i·	→	D		k_{tc}^{SS}

However, in the copolymerization case (Scheme 5), chain transfer to polymer can be regarded negligible if not nonexistent.[22] Thus, the equilibrium involving chains with *n*-butyl acrylate terminal units (reactions 4 and 5 in Scheme 5) are governed by the rate coefficients that govern reaction (1) in Scheme 4. The use of the equilibrium kinetic parameters determined from homopolymerization (with chain transfer to polymer present), can thus introduce an inaccurate description of the copolymerization process (Figures 6 and 7).

Parameter estimation (PE) studies with the Predici software package were then carried out to determine the optimum values of k_c^B and k_d^B for which the model would fit the experimental data in the feed composition range studied.

The results of the PE study are summarized in Table 2. These optimum values were then adapted into the model to replace the values indicated in Table 1 for further modeling studies of the copolymerization process. Figures 8−11 illustrate the evolution of both styrene and *n*-butyl acrylate concentrations with time, at two feed compositions. An improved correlation between experimental and simulated data was observed in the feed composition

Table 1. Rate Parameters Used in the Simulation of the Nitroxide-Mediated Copolymerization of Styrene and *n*-Butyl Acrylate As Depicted in Scheme 3

coefficient	A	E (kJ/mol)	Value (120 °C)	refs
k_{act}	2.4×10^{14} s^{-1}	112.3	0.289 s^{-1}	12
k_{deact}			5.0×10^{6} L mol^{-1} s^{-1}	13
k_{add}^{S}	6.7×10^{6} L mol^{-1} s^{-1}	16.5		13, 14
k_{add}^{B}	4.0×10^{6} L mol^{-1} s^{-1}	19.8		13, 14
k_{p}^{SS}	4.27×10^{7} L mol^{-1} s^{-1}	32.5		15
k_{p}^{BB}	2.31×10^{7} L mol^{-1} s^{-1}	18.1		16
r_S			0.74	this work[a]
r_B			0.23	this work[a]
s_S			0.48	17
s_B			0.06	17
k_{c}^{S}			2.6×10^{5} L mol^{-1} s^{-1}	13
k_{d}^{S}			7.5×10^{-3} L mol^{-1} s^{-1}	13
k_{c}^{B}			2.8×10^{7} L mol^{-1} s^{-1}	13, 18
k_{d}^{B}			1.55×10^{-3} L mol^{-1} s^{-1}	13
k_{tc}^{SS}			1.8×10^{8} L mol^{-1} s^{-1}	13
k_{tc}^{BB}			7.34×10^{7} L mol^{-1} s^{-1}	13
k_{tc}^{SB}			1.0×10^{8} L mol^{-1} s^{-1}	estimate

[a] The reactivity ratios of styrene and *n*-butyl acrylate were estimated from the high conversion in situ ^{1}H NMR data following the method described by Aguilar et al.[8]

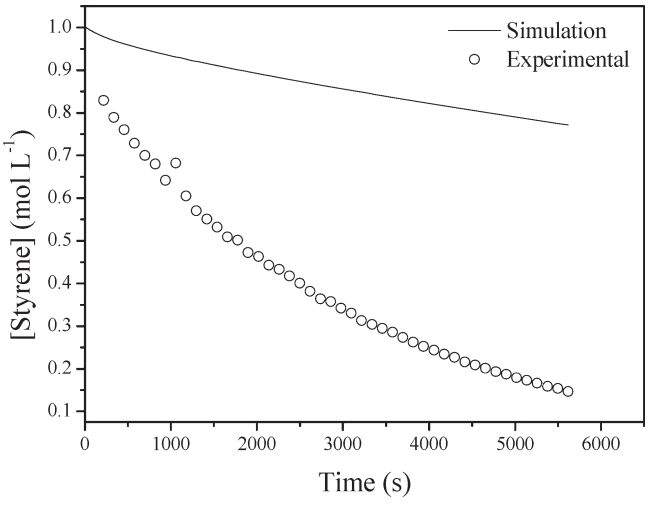

Figure 6. Simulated vs experimental evolution of styrene concentration with time for $f_S^0 = 0.3$. k_c^B and k_d^B values used in the simulation are in Table 1.

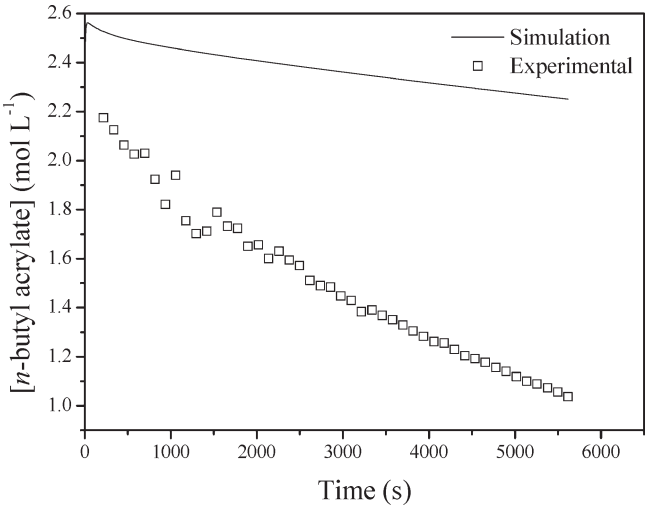

Figure 7. Simulated vs experimental evolution of *n*-butyl acrylate concentration with time for $f_S^0 = 0.3$. k_c^B and k_d^B values used in the simulation are in Table 1.

range studied when the values of k_c^B and k_d^B determined from the PE study were used. Figures 8 and 9 illustrate the agreement between the model and experiments below the azeotropic feed composition of the styrene/*n*-butyl acrylate system, while Figures 10 and 11 show the agreement above the azeotropic feed composition.

To further probe how representative the proposed model is of the real copolymerization system, simulations were carried out to predict the terminal unit of dormant chains. Figures 12 and 13 illustrate the evolution of fraction of dormant chains which possess *n*-butyl acrylate as the terminal unit at two different initial feed compositions. Even though the ^{31}P NMR were marked by overlap of peaks from dormant chains with styrene and *n*-butyl acrylate as terminal units, the method of analysis used to separate both signals resulted in data that is comparable with the simulation data from the proposed model.

A reasonable quantitative agreement is observed between model and experimental data. However, a fairly poor qualitative agreement between the model and experimental data is observed, with the greatest deviation at early reaction times. This deviation can be ascribed to the uncertainties in the approximated rate coefficients of first monomer addition (k_{add}^S and k_{add}^B). The actual values of the rate coefficients of addition of styrene and *n*-butyl acrylate to the 2-carboxyprop-2-yl radical are not known. But

dx.doi.org/10.1021/ma2011624 |*Macromolecules* 2011, 44, 6683–6690

Scheme 4. Two Equilibrium Reactions in the Nitroxide-Mediated *n*-Butyl Acrylate Homopolymerization Involving both the Secondary Propagating Radical (SPR, Represented by P) and the Tertiary Mid-Chain Radical (MCR, Represented by Q) with the Nitroxide Represented by Y

SPR NMP Equilibrium

$$P_i\cdot + Y \underset{k_d^B}{\overset{k_c^B}{\rightleftharpoons}} P_i\text{-}Y \qquad (1)$$

MCR NMP Equilibrium

$$Q_i\cdot + Y \underset{k_d^t}{\overset{k_c^t}{\rightleftharpoons}} Q_i\text{-}Y \qquad (2)$$

Scheme 5. NMP Equilibrium Reactions Involving the Chains with *n*-Butyl Acrylate Terminal Unit in Nitroxide-Mediated Copolymerization of *n*-Butyl Acrylate and Styrene Considering the Penultimate Unit Model

$$PSB_i\cdot + Y \underset{k_d^B}{\overset{k_c^B}{\rightleftharpoons}} PSB_i\text{-}Y \qquad (4)$$

$$PBB_i\cdot + Y \underset{k_d^B}{\overset{k_c^B}{\rightleftharpoons}} PBB_i\text{-}Y \qquad (5)$$

Table 2. Optimum Values of k_c^B and k_d^B Obtained from the Parameter Estimation Study

coefficient	optimum value	95% confidence interval
k_c^B	5×10^5	$\pm 1 \times 10^5$
k_d^B	7×10^{-4}	$\pm 1 \times 10^{-4}$

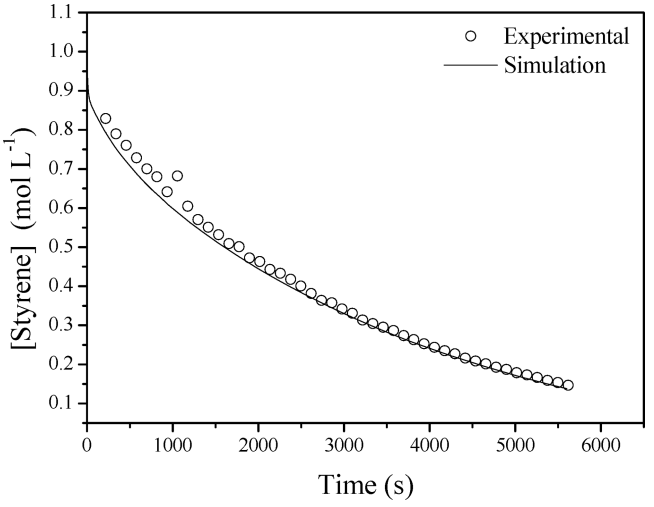

Figure 8. Simulated and experimental evolution of styrene concentration with time for $f_S^0 = 0.3$. k_c^B and k_d^B values used are 5×10^5 L mol^{-1} s^{-1} and 7×10^{-4} s^{-1}, respectively.

these rate coefficients are believed to be close to those of addition of similar monomers to 2-(alkoxy)carboxyprop-2-yl radical utilized in the model.[13] The selectivity of the primary radical for

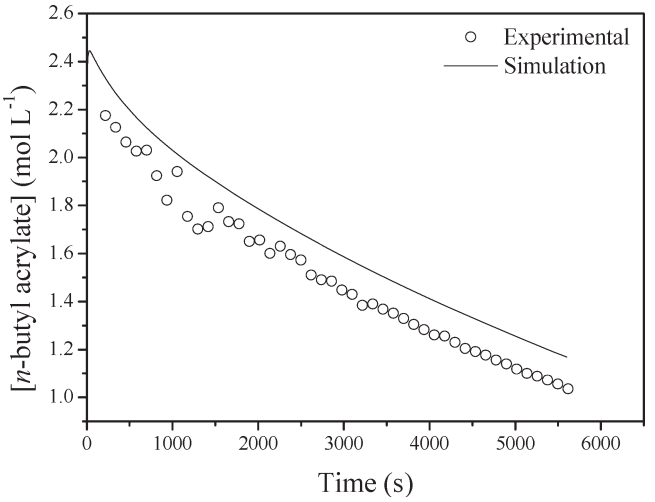

Figure 9. Simulated and experimental evolution of *n*-butyl acrylate concentration with time for $f_S^0 = 0.3$. k_c^B and k_d^B values used are 5×10^5 L mol^{-1} s^{-1} and 7×10^{-4} s^{-1}, respectively.

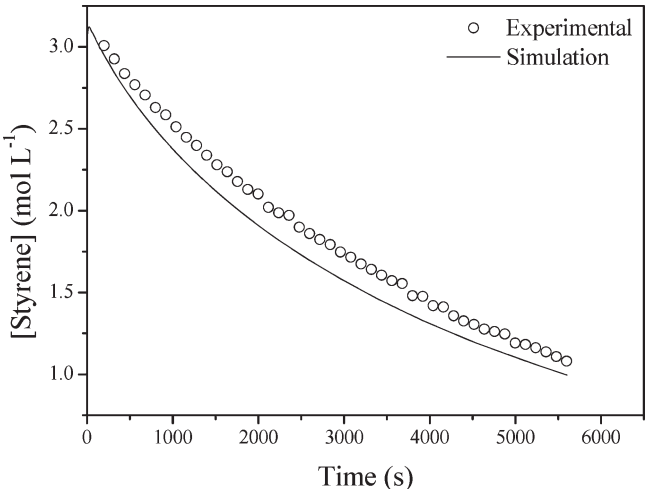

Figure 10. Simulated and experimental evolution of styrene concentration with time for $f_S^0 = 0.8$. k_c^B and k_d^B values used are 5×10^5 L mol^{-1} s^{-1} and 7×10^{-4} s^{-1}, respectively.

addition to styrene and *n*-butyl acrylate, governed by the rate coefficients of addition of the respective monomers, will determine the fraction of each respective dormant species, before the steady-state conditions are attained. This will occur until such a point that the radical ratio in the copolymerization system is governed by the reactivity ratios.

Further improvements of the model are however required, on both the qualitative and quantitative description of the copolymerization system with respect to the terminal unit of the dormant chains. In the Supporting Information further extensions to the parameter estimation studies are considered, with prime interest in improving the qualitative description of the fraction of dormant chains with either styrene or *n*-butyl acrylate as the terminal unit to which the nitroxide is attached. It turns out that the simultaneous parameter estimation of four rate parameters does not lead to a unique solution. Although the quality of the fit to the experimental data improves, it is difficult to judge what the physical relevance of the parameters is.

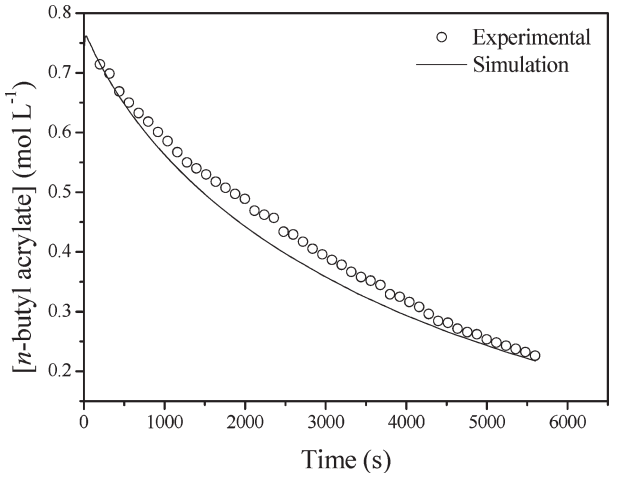

Figure 11. Simulated and experimental evolution of *n*-butyl acrylate concentration with time for $f_S^0 = 0.8$. k_c^B and k_d^B values used are 5×10^5 L mol^{-1} s^{-1} and 7×10^{-4} s^{-1}, respectively.

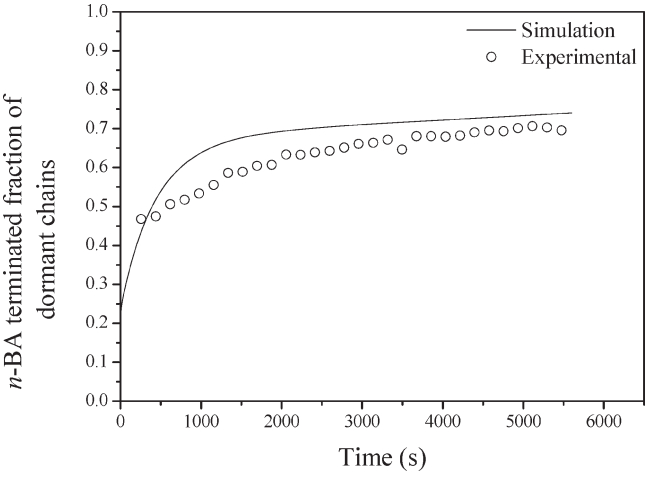

Figure 12. Experimental and simulated fractions (as a function of time) of dormant chains with *n*-butyl acrylate as the terminal unit in the copolymerization of styrene and *n*-butyl acrylate with $f_S^0 = 0.29$.

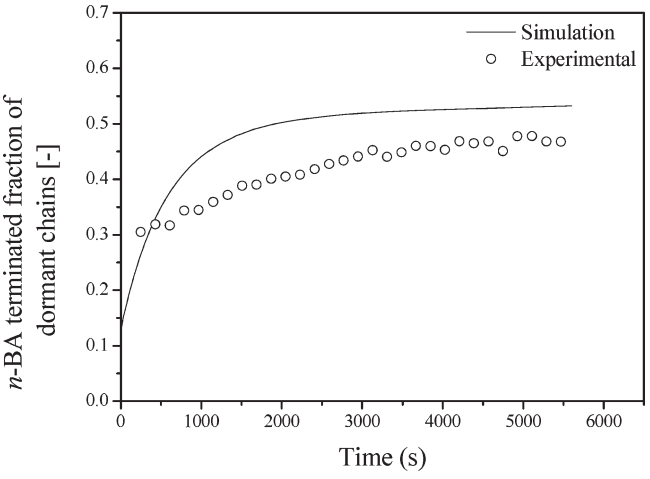

Figure 13. Experimental and simulated fractions (as a function of time) of dormant chains with *n*-butyl acrylate as the terminal unit in the copolymerization of styrene and *n*-butyl acrylate with $f_S^0 = 0.58$.

CONCLUSION

In situ ^{1}H and ^{31}P NMR monitored copolymerizations of styrene and *n*-butyl acrylate were successfully carried out. The copolymer composition curve was constructed from the *in situ* ^{1}H NMR data and was found to be in good agreement with a curve predicted from the reactivity ratios determined in this study. The terminal units of dormant polymer chains were profiled as a function of polymerization time via *in situ* ^{31}P NMR. The values of the rate coefficients describing the equilibrium involving the *n*-butyl acrylate terminal unit (k_c^B and k_d^B) were determined by fitting (via the parameter estimation tool of the Predici software package) the model to data extracted from *in situ* ^{1}H NMR experiments. The obtained values of k_c^B and k_d^B resulted in good agreement between the model and experimental data in the initial feed composition range studied. The resulting model also yielded good agreement between simulations and (dormant chain) terminal unit data extracted from *in situ* ^{31}P NMR experiments.

ASSOCIATED CONTENT

Supporting Information. Synthetic procedure for the synthesis of the alkoxyamine MAMA-DEPN including the ^{1}H NMR spectrum, analysis of the *in situ* ^{31}P NMR data, and simulation of styrene/BA copolymerization with PREDICI. This material is available free of charge via the Internet at http://pubs.acs.org

AUTHOR INFORMATION

Corresponding Author
*E-mail: bklump@sun.ac.za.

ACKNOWLEDGMENT

The authors thank Heidi Assumption and Elsa Malherbe for assistance with *in situ* NMR experiments. The authors would like to acknowledge Stellenbosch University and the South African Research Chairs Initiative (SARChI) from DST and NRF for financial support.

REFERENCES

(1) Arehart, S. V.; Matyjaszewski, K. *Macromolecules* **1999**, *32*, 2221–2231.
(2) Barner-Kowollik, C.; Heuts, J. P. A.; Davis, T. P. *J. Polym. Sci., Part A: Polym. Chem.* **2001**, *39*, 656–664.
(3) Börner, H. G.; Kühnle, H.; Hentschel, J. *J. Polym. Sci., Part A: Polym. Chem.* **2010**, *48*, 1–14.
(4) Hawker, C. J.; Elce, E.; Dao, J.; Volksen, W.; Russell, T. P.; Barclay, G. G. *Macromolecules* **1996**, *29* (7), 2686–2688.
(5) Benoit, D.; Grimaldi, S.; Robin, S.; Finet, J.-P.; Tordo, P.; Gnanou, Y. *J. Am. Chem. Soc.* **2000**, *122*, 5929–5939.
(6) Ziaee, F.; Nekoomanesh, M. *Polymer* **1998**, *39* (1), 203–207.
(7) Pound, G.; McLeary, J. B.; McKenzie, J. M.; Lange, R. F. M.; Klumperman, B. *Macromolecules* **2006**, *39*, 7796–7797.
(8) Aguilar, M. R.; Gallardo, A.; Fernández, M. d. M.; Román, J. S. *Macromolecules* **2002**, *35* (6), 2036–2041.
(9) Abdollahi, M.; Mehdipour-Ataei, S.; Ziaee, F. *J. Appl. Polym. Sci.* **2007**, *105*, 2588–2597.
(10) Barner, L.; Barner-Kowollik, C.; Davis, T. P. *J. Polym. Sci., Part A: Polym. Chem.* **2002**, *40*, 1064–1074.
(11) Kelemen, P.; Klumperman, B. *Macromolecules* **2004**, *37*, 9338–9344.
(12) Bertin, D.; Gigmes, D.; Marque, S. R. A.; Tordo, P. *Macromolecules* **2005**, *38*, 2638–2650.

(13) Chauvin, F.; Dufils, P.-E.; Gigmes, D.; Guillaneuf, Y.; Marque, S. R. A.; Tordo, P.; Bertin, D. *Macromolecules* **2006**, *39*, 5238–5250.
(14) Zytowski, T.; Knühl, B.; Fischer, H. *Helv. Chim. Acta* **2000**, *83*, 658–675.
(15) Beuermann, S.; Buback, M. *Prog. Polym. Sci.* **2002**, *27* (2), 191–254.
(16) Barner-Kowollik, C.; Günzler, F.; Junkers, T. *Macromolecules* **2008**, *41*, 8971–8973.
(17) Chambard, G. Ph.D. Thesis, Technische Universiteit Eindhoven, Eindhoven, The Netherlands, 2000.
(18) Chauvin, F.; Alb, A. M.; Bertin, D.; Tordo, P.; Reed, W. F. *Macromol. Chem. Phys.* **2002**, *203* (14), 2029–2041.
(19) Willemse, R. X. E.; Herk, A. M. v.; Panchenko, E.; Junkers, T.; Buback, M. *Macromolecules* **2005**, *38*, 5098–5103.
(20) Nikitin, A. N.; Hutchinson, R. A.; Buback, M.; Hesse, P. *Macromolecules* **2007**, *40*, 8631–8641.
(21) Junkers, T.; Koo, S. P. S.; Davis, T. P.; Stenzel, M. H.; Barner-Kowollik, C. *Macromolecules* **2007**, *40*, 8906–8912.
(22) Hlalele, L.; Klumperman, B. *Macromolecules* **2011**, *44*, 5554–5557.